

## Original Article

## Root cortical senescence decreases root respiration, nutrient content and radial water and nutrient transport in barley

Hannah M. Schneider<sup>1</sup>, Tobias Wojciechowski<sup>1</sup>, Johannes A. Postma<sup>1</sup>, Kathleen M. Brown<sup>2</sup>, Andreas Lücke<sup>3</sup>, Viktoria Zeisler<sup>4</sup>, Lukas Schreiber<sup>4</sup> & Jonathan P. Lynch<sup>2</sup> 

<sup>1</sup>Forschungszentrum Jülich, Institut für Bio- und Geowissenschaften Pflanzenwissenschaften (IBG-2), 52428 Jülich, Germany, <sup>2</sup>Department of Plant Science, The Pennsylvania State University, University Park, State College, PA 16802, USA, <sup>3</sup>Forschungszentrum Jülich, IBG-3: Agrosphere, 52428 Jülich, Germany and <sup>4</sup>Department of Ecophysiology, Institute of Cellular and Molecular Botany, University of Bonn, Kirschallee 1D-53115 Bonn, Germany

## ABSTRACT

**The functional implications of root cortical senescence (RCS) are poorly understood. We tested the hypotheses that RCS in barley (1) reduces the respiration and nutrient content of root tissue; (2) decreases radial water and nutrient transport; and (3) is accompanied by increased suberization to protect the stele. Genetic variation for RCS exists between modern germplasm and landraces. Nitrogen and phosphorus deficiency increased the rate of RCS. Maximal RCS, defined as the disappearance of the entire root cortex, reduced root nitrogen content by 66%, phosphorus content by 63% and respiration by 87% compared with root segments with no RCS. Roots with maximal RCS had 90, 92 and 84% less radial water, nitrate and phosphorus transport, respectively, compared with segments with no RCS. The onset of RCS coincided with 30% greater aliphatic suberin in the endodermis. These results support the hypothesis that RCS reduces root carbon and nutrient costs and may therefore have adaptive significance for soil resource acquisition. By reducing root respiration and nutrient content, RCS could permit greater root growth, soil resource acquisition and resource allocation to other plant processes. RCS merits investigation as a trait for improving the performance of barley, wheat, triticale and rye under edaphic stress.**

*Key-words:* *Hordeum vulgare*; radial transport; suberin.

*List of Abbreviations:* DAG, days after germination; DW, dry weight; LN, low nitrogen; LP, low phosphorus; RCA, root cortical aerenchyma; RCS, root cortical senescence; VSMOW, Vienna Standard Mean Ocean Water

## INTRODUCTION

Efficient acquisition of soil resources is key in improving plant performance. Root traits that reduce respiration and nutrient content, including RCA, cortical cell size and cortical cell file number, convert living cortical parenchyma into air space and thereby reduce carbon and nutrient costs for soil exploration

(Lynch, 2013, 2015; Lynch *et al.*, 2014). Several studies have demonstrated that the reduction in living root cortical area may improve water and nutrient acquisition under drought and other edaphic stresses (Zhu *et al.*, 2010; Postma and Lynch, 2011a,b; Jaramillo *et al.*, 2013; Saengwilai *et al.* 2014; Chimungu *et al.*, 2014a,b). We hypothesize that the development of RCS, resulting in a reduction in living cortical area, is an adaptive response under edaphic stresses by reducing the carbon and nutrient costs of soil exploration.

Root cortical senescence in Triticeae is formed by programmed cell death of root cortical cells. RCS is distinctly different than the loss of the root cortex because of secondary root growth in many dicotyledonous plants (Bingham, 2007), and studies have suggested that RCS is a distinct process from RCA formation (Deacon *et al.*, 1986). During the formation of RCS, cortical cells of seminal roots senesce early in plant growth (Henry and Deacon, 1981; Deacon and Mitchell, 1985). RCS begins in the outer cortical cell files, directly behind the zone of anucleate root hairs, and progresses inwards resulting in anucleate cortical cells. Anucleate cortical cells are indicative of RCS. Root cortical cells undergo senescence increasing in frequency basipetally, and eventually, all cortical cells will become anucleate. Cell layers around the base of the lateral roots typically do not undergo RCS, or senescence is delayed even though the lateral branches themselves eventually undergo cortical senescence (Henry and Deacon, 1981). In 15-day-old regions of barley (*Hordeum vulgare*) seminal roots grown in soil, between 20 and 35% of root cortical cells were anucleate (Liljeroth, 1995).

The literature presents conflicting results on the effect of N, P and K supply on the development of RCS in wheat (*Triticum aestivum*). The rate of RCS was accelerated by severe, but not moderate, N deficiencies (Lascaris and Deacon, 1991) and accelerated with ammonium, but not nitrate application (Brown and Hornby, 1987; Gillespie and Deacon, 1988). In one study, the supply of ammonium nitrogen affected the pattern, but not the fraction of anucleate cortical cells (Elliott *et al.*, 1993). Gillespie and Deacon (1988) showed that P and K deficiencies had little effect on the rate of RCS. However, in contrast, RCS was accelerated by moderate, but not severe, P deficiencies, and the supply of P influenced the pattern of

*Correspondence:* J. P. Lynch; e-mail: jpl4@psu.edu

RCS (Elliott *et al.*, 1993). However, many of these studies have several drawbacks and investigate a limited number of root classes, young plants or roots on agar plates. The effect of mineral nutrient deficiencies on the rate and pattern of RCS remains unclear. In the present study, we examine the development of RCS in seminal and nodal roots in low-P and low-N conditions.

We propose that the function of RCS may be similar to that of RCA formation in maize in response to drought or nutrient deficiency (not hypoxia where RCA may function differently). RCA has been shown to reduce uptake of sulphate, calcium and phosphate in whole maize plants (Hu *et al.*, 2014) and reduce root radial hydraulic conductivity in maize roots under low-P conditions (Fan *et al.*, 2007). The formation of intercellular lacunae in cortical cells of desert agave decreased radial water conductivity in the root cortex (Huang and Nobel, 1994; North and Nobel, 1995). The development of RCS may reduce radial water transport through cell-to-cell and apoplastic pathways resulting in a longer path length, eliminating the continuity of the cell-to-cell pathway, and reduced cross-sectional area for transport across these pathways in the cortex. It is estimated that 70 to 90% of resistance to radial water flow is due to cell types external to mature xylem vessels (Steudle and Peterson, 1998), and of these cell types, suberized epidermis/exodermis and endodermis have the lowest conductance for radial water transport (North and Nobel, 1995, 1996). The conductance of the endodermis depends on the development of the Casparian strip and suberin lamellae (Sanderson, 1983; Passioura, 1988; Peterson *et al.*, 1993; North and Nobel, 1995). The suberin lamellae prevent water loss from the root to dry soil and may help protect against pathogen invasion (Enstone *et al.*, 2003). Once RCS has occurred, breaks in the epidermis and a senesced cortex leave the root prone to radial water loss and pathogen invasion. Increased suberization of the endodermis may be a mechanism during the progression of RCS to reduce radial water loss and pathogen invasion.

The functional implications of RCS formation are poorly understood. The objectives of this research were to test the hypotheses that RCS (1) decreases the carbon and nutrient costs of barley root tissue; (2) decreases radial water and nutrient transport; and (3) is accompanied by increased suberization. The few previous studies on RCS have exclusively focused on the formation of RCS and its association with disease. To our knowledge, we present the first quantitative evaluation of the spatial and temporal development of RCS. We present the first evidence of RCS in nodal roots and the association of RCS with changes in radial water and nutrient transport, suberization of the endodermis, root respiration and nutrient content of the root.

## MATERIALS AND METHODS

### Barley genotypes

Four barley genotypes (two landraces, Nuernburg and Tkn24b, and two modern varieties, Arena and Golf) were

selected based on contrasting RCS formation in preliminary screening studies. Seeds were obtained from IPK, Gatersleben (Gatersleben, Germany). Tkn24b originated in Nepal; Nuernburg and Arena are from Germany; and Golf is from the United Kingdom.

## Growth systems

### *Rhizotron in greenhouse*

Four barley seeds were sown directly in rhizotrons (90 × 60 × 3.4 cm) in eight replications per genotype. The rhizotrons, consisting of a black polyethylene back plate with sides and one transparent polycarbonate plate, were filled with peat-based substrate (pH 6). Plants were grown in the PhyTec greenhouse of the Institute Plant Sciences (IBG-2; Forschungszentrum Jülich GmbH, Jülich, Germany) at a daylength of 16 h and day/night temperatures of ~24/18 °C. Agro high-pressure sodium lamp supplemental illumination (SON-T AGRO 400, Philips, Amsterdam, The Netherlands) was provided to keep the light intensity >300 μmol photons m<sup>-2</sup> s<sup>-1</sup>. To keep the soil water content at a minimum of 30% volumetric water content and to ensure sufficient water supply, plants were watered every other day with 250 mL of deionized water and watered with an additional 50 mL nutrient solution (solution culture composition in the following) every 5 d. At 35 DAG, roots were harvested by removing the transparent plate and then washed with low-pressure water, sampled, preserved in 70% ethanol and stained with acridine orange for anatomical analysis. Root segments (1 cm length) were sampled at nine positions on seminal roots (6, 12, 18, 24, 30, 36, 42, 48 and 54 cm from the apex) and at four positions on nodal roots (3, 8, 13 and 18 cm from the apex).

### *Solution culture in climate chamber*

Seeds were surface-sterilized in 1.5% NaOCl in water, transferred to germination paper (76 lb, Anchor Paper, St Paul, MN, USA), then rolled into tubes and stood in covered beakers containing 0.5 mM CaSO<sub>4</sub> at 28 °C for 4 d in a dark climate chamber. The rolls containing germinated seedlings were then placed under a fluorescent light (350 μE m<sup>-2</sup> s<sup>-1</sup>) for 1 d before transplanting into aerated solution culture. Five seedlings were transferred to randomly assigned foam plugs suspended above each 33 L solution culture tank in a climate chamber (22 °C, 12 h daylight, 50% RH) for 30 d. The nutrient solution (pH 5.5) contained 2.5 mM KNO<sub>3</sub>, 2.5 mM Ca(NO<sub>3</sub>)<sub>2</sub>, 1 mM MgSO<sub>4</sub>, 0.5 mM KH<sub>2</sub>PO<sub>4</sub>, 50 μM NaFeEDTA, 0.2 μM Na<sub>2</sub>MoO<sub>4</sub>, 10 μM H<sub>3</sub>BO<sub>3</sub>, 0.2 μM NiSO<sub>4</sub>, 1 μM ZnSO<sub>4</sub>, 2 μM MnCl<sub>2</sub>, 0.5 μM CuSO<sub>4</sub> and 0.2 μM CoCl<sub>2</sub>. The pH of the nutrient solution was adjusted daily to 5.5 with KOH, and the complete solution replaced every 7 d. Nitrate and phosphate concentration were tested twice weekly using kits (phosphate: LCK350; nitrate: LCK340, Hach Lange) measured spectrophotometrically (Dr 500, Hach Lange, Dusseldorf, Germany).

## Measurement of root cortical senescence

### *Root cortical senescence rate studies*

To determine the rate of RCS formation in nutrient deficient conditions, barley genotypes were grown under control, LN (200  $\mu\text{mol N L}^{-1}$ ) and low alumina-buffered phosphorus (LP) (buffered at 2  $\mu\text{mol P L}^{-1}$ ) (Lynch *et al.*, 1990) conditions in solution culture. In the case of LN conditions, the  $\text{KNO}_3$  and  $\text{Ca}(\text{NO}_3)_2$  were reduced from the nutrient solution and supplemented with  $\text{K}_2\text{SO}_4$  and  $\text{CaCl}_2$  to maintain 2.5 mM  $\text{Ca}^{2+}$  and 3 mM  $\text{K}^+$ . In LP conditions,  $\text{KH}_2\text{PO}_4$  was replaced with  $\text{K}_2\text{SO}_4$  and alumina-buffered phosphorus to maintain 3 mM  $\text{K}^+$  and achieve low levels of P. Eight harvests were conducted at 5 d intervals from 10 to 45 DAG. Dry plant biomass and root length of individual roots were collected. In three replications, seven positions were sampled on seminal roots (2, 6, 15, 25, 35 and 45 cm from the apex and 2 cm from the seed) and six positions were sampled on nodal roots (2, 4, 10, 15 and 20 cm from the apex and 2 cm from the seed) and preserved in 70% ethanol.

### *Acridine orange staining and anatomical characterization*

Root segments preserved in 70% ethanol were stained with acridine orange for anatomical analysis. Acridine orange staining has been determined to be a viable method to assess RCS. This method has been used in literature to phenotype RCS and correlates with other methods of assessing cell viability including Feulgen staining (Henry and Deacon, 1981) and single cell pressure probe methods (Bingham, 2007). Acridine orange fluorescent nuclei were used to phenotype the onset of RCS within individual cortical layers. The disappearance of the cortex, as determined by a percentage of viable cells (described in the following), was used to phenotype RCS on a root cross-sectional level. Acridine orange staining was performed according to Henry and Deacon (1981); however, the staining time was extended to 30 min. Stained roots were embedded in a gelatin capsule with Tissue-Tek CRYO-OCT compound (Fisher Scientific, Massachusetts, USA), and transverse sections 60  $\mu\text{m}$  thick were cut using a Kryostat 2800 Frigocut -E (Reichert-Jung, Leica Instruments GmbH, Nussloch, Germany). Images of cross sections were acquired on a compound microscope (Zeiss Axioplan 2, mounted with an AxioCam ICc 5, Filter 09: Blue 450–490 nm Carl Zeiss Jena GmbH, Jena, Germany; 20 $\times$  magnification) for mannitol and radial water loss experiments. All other root cross sections were imaged on a confocal microscope (Nikon, Eclipse C1, Nikon, Japan, 450 nm filter, 20 $\times$  magnification).

Root cross sections were analysed for root cross-sectional area and diameter, area of the stele, diameter of the stele, area, count and diameter of individual meta xylem vessels and the number of acridine orange fluorescent nuclei in the inner, middle and outer cortical regions. The number of acridine orange-stained fluorescent nuclei was counted in all cell layers of the 60  $\mu\text{m}$  thick section. In selected experiments, root segments were collected 3 cm from the root apex in

addition to the sample position. These segments are a reference for root cortical area in regions with no RCS on the same root. For root segments collected at the 3 cm from the root apex reference point, root cross sections were phenotyped for cross-sectional diameter and area, area of the stele, number of cortical cell files and number of acridine orange-stained fluorescent nuclei in the inner, middle and outer cortical regions. Root anatomical features were phenotyped using ImageJ (Rasband 1997). Percent cortex senesced was calculated based on the difference in cross-sectional areas (total cross-sectional area minus stele area) at 3 cm from the root apex and at the sample position. Surface area of the exposed root segment in the Pitman chamber was estimated as the outer surface area of a tube, with the length determined by the length of the compartment, and the radius was calculated from the cross-sectional diameter. For the  $^{32}\text{P}$  experiments, root hair length and density were measured using a compound microscope (DigiMicro 2.0, dnt, Dietzenbach, Germany). Surface area of individual root hairs and lateral roots were estimated as the outer surface area of a tube.

In order to normalize fluorescent nuclei counts in different regions of the cortex to a 60  $\mu\text{m}$  thick section, we quantified cell lengths in different cortical regions. To determine cell length, barley genotypes were grown in three replicates and sampled at three positions (5, 10 and 20 cm from the apex) on seminal and nodal roots. Samples were preserved in 70% ethanol and stained with acridine orange for anatomical analysis. Cell length was determined by cutting longitudinal sections, 60  $\mu\text{m}$  thick, and measuring cell length in three cortical regions (inner, middle and outer cortex). These three cortical regions were determined by dividing the total number of cortical cell files in three equal radial parts. Using the cell length data, for all experiments, fluorescent acridine orange-stained nuclei counts per cortical cell region were normalized to a 60  $\mu\text{m}$  thick section. The average cell length per cortical region and root class was divided by 60  $\mu\text{m}$ . The number of fluorescent nuclei in each cortical region was multiplied by this factor to obtain corrected nuclei counts. The outer regions had cell lengths 44 and 22% longer than the inner and middle regions, respectively.

## Root activity

### *Root respiration*

Root respiration was measured in eight replicates for each genotype and sample position from solution culture grown plants at 35 DAG. Respiration was measured by excising a root segment (2 cm in length) for each sample position and immediately suspending the segment in 1 mL of nutrient solution and transferring into a liquid phase oxygen electrode chamber (Hansatech Instruments Ltd, United Kingdom). The rate of root respiration was measured over 5 min. After root respiration measurements, the root segment was dried and weighed. A 5 mm root segment directly basally adjacent to the sampled root was preserved in 70% ethanol and stained with acridine orange for anatomical analysis.

### Root nutrient content

To determine how RCS influences the nutrient content of root tissue, we measured N and P tissue content in root segments with different degrees of RCS formation. Two genotypes (Arena and Nuernburg) were grown in two replications in three treatments (LN, LP and control conditions, described previously) in solution culture. At 35 DAG, 4 cm segments of seminal and nodal roots were sampled at three positions relative to the root apex [6–10 cm (distal), 20–24 cm (mid-root) and 34–38 cm (basal)]. These sample positions were chosen according to RCS formation; the distal segment had no RCS, the mid root segment had progressing RCS and the basal section had maximal RCS defined as complete disappearance of the cortex. Nitrogen content of root tissue was determined using an elemental analyser (Series II CHNS/O Analyser 2400, Perkin Elmer, Massachusetts, USA). For P analysis, tissue was ashed at 500 °C for 14 h, dissolved in 5 N H<sub>2</sub>SO<sub>4</sub>, and P content determined spectrophotometrically (Murphy and Riley, 1962). In addition, root segments (1 cm in length) directly basally adjacent to sample positions were collected, preserved in 70% ethanol and stained with acridine orange for anatomical analysis.

### Transport activity

#### Radial water and nitrate transport

These experiments measured the radial transport of H<sub>2</sub><sup>18</sup>O and N<sup>18</sup>O<sub>3</sub> in excised roots. The purpose of these experiments was to determine how RCS formation affected radial water and nutrient transport. The Pitman chamber enables the measurement of transport in an isolated segment of an excised root based on differences in osmotic pressure between the nutrient solution and the xylem. From a solution culture grown plant at 35 DAG, a root was excised, and its length measured. The root was trimmed at the excised end to 1 cm from the sample position and installed in a modified Pitman chamber (Hu *et al.*, 2014) (Fig. 1a) permitting treatment of a segment of root (in this case, 5 mm) with <sup>18</sup>O enriched water or nitrate. The length of root in the Pitman chamber varied between sample locations; however, the length of root exposed to the treatment compartment and the length of root between the treatment and receiver compartment remained consistent. The Pitman chamber was placed in a water bath at 22 °C to stabilize the temperature. A 1 cm segment of root extended from the 200 μL treatment compartment to the 300 μL receiver compartment. Silicon grease (Dow Corning, Midland, MI, USA) was used to isolate the compartments. Nutrient solution at pH 6.0 was added to the treatment compartment, the receiver compartment and the space around the root tip. Ten minutes after excision, the solution in the treatment compartment was replaced with fresh agar gel containing nutrient solution with an enriched oxygen isotope composition with a δ<sup>18</sup>O value of 56.77 per mil versus VSMOW for H<sub>2</sub><sup>18</sup>O experiments and 57.77 δ<sup>18</sup>O versus VSMOW for N<sup>18</sup>O<sub>3</sub> experiments. The gel was placed in the treatment compartment to avoid contact with lateral roots. A gel was used instead of a liquid solution, so the

isotope could be fully in contact with the axial root and avoid any contact with lateral roots. We were interested in the effect of RCS on radial transport of the axial root, and any exposure of the lateral roots in the treatment compartment would negate the results. The chamber was covered with a plexiglass plate to prevent evaporation. After 20 min, the solution in the receiver compartment was replaced with 250 μL nutrient solution. After 10 min, the entire solution in the receiver compartment was collected and weighed on an analytical balance (±0.1 μg). The remaining solution in the treatment compartment was collected and weighed. Exuded xylem sap and nutrient solution in the Pitman chamber were collected and analysed to determine osmolality (Fiske Micro-Osmometer, Model 210, Fiske Associates, Massachusetts, USA). Sample times for Pitman chamber experiments were determined by separate time course experiments sampling the receiver compartment 13 times at 5 min intervals (Fig. S1a,b).

Upon the completion of the experiment, the solution in the leakage check compartment (compartment adjacent to treatment compartment) was replaced with 0.05% toluidine blue (Sigma-Aldrich, Taufkirchen, Germany) for 4 min to detect leakage between compartments. Leakage between compartments could be detected by movement of the toluidine blue to the receiver or treatment chambers; data from chambers showing any leakage were discarded. There were eight replicates for each 5 mm root segment exposed to the treatment compartment for each genotype and individual sample position for both H<sub>2</sub><sup>18</sup>O and N<sup>18</sup>O<sub>3</sub> experiments. Root segments (5 mm in length) exposed to the treatment compartment were excised and stored in 70% ethanol for acridine orange staining and anatomical analysis. In addition, a 1 cm root segment was sampled 3 cm from the apex of each individual root installed in the Pitman chamber. This root sample was used as a reference for anatomical traits with no RCS development in the same root. Solution samples from the receiver compartment collected from 20 to 30 min after treatment were stored at 4 °C and analysed for <sup>18</sup>O content. Water isotope analyses were carried out using cavity ring down spectroscopy (CRDS, L2130i, Picarro Inc., California, USA). Results are reported as δ values in per mil (‰), where  $\delta = (R_S/R_{St} - 1) * 1000$  with R<sub>S</sub> and R<sub>St</sub> as isotope ratios (<sup>18</sup>O/<sup>16</sup>O) of samples and standards, respectively. δ<sup>18</sup>O values are reported relative to VSMOW water (Brand *et al.*, 2014). Internal standards calibrated against VSMOW, Standard Light Antarctic Precipitation and Greenland Ice Sheet Precipitation were used for calibration and to ensure long-term stability of analyses. The precision of the analytical system was ≤0.1‰ for δ<sup>18</sup>O and ≤0.5‰ for δ<sup>2</sup>H.

#### Radial phosphate transport

This experiment was performed to measure the radial transport of <sup>32</sup>P in excised roots to determine the association between RCS and radial phosphorus transport. From a solution culture grown plant at 35 DAG, a root was excised and measured for length and scored for lateral branching density and length at the sample position. The root was trimmed to the appropriate size from the excised end (3 cm from sample

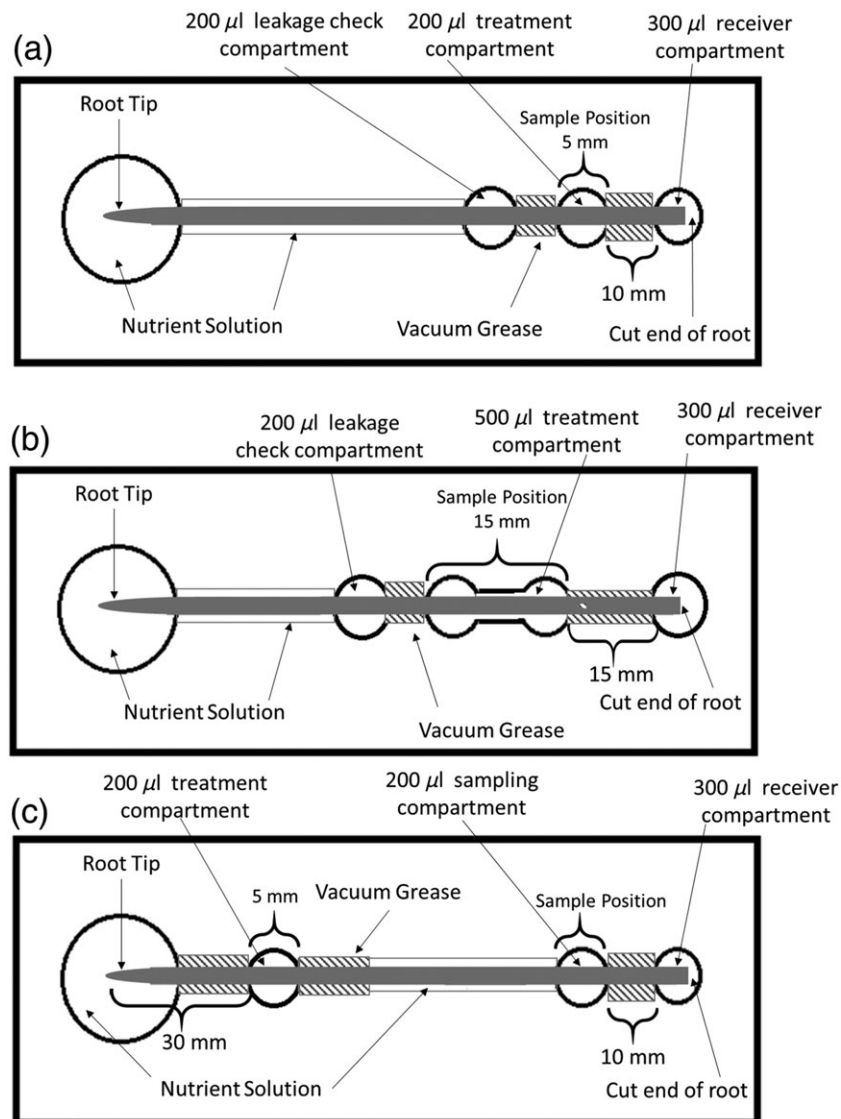


**Figure 1.** Experimental set-up for Pitman chamber experiments. (a) H<sub>2</sub><sup>18</sup>O and N<sup>18</sup>O<sub>3</sub> experiments. A modified Pitman chamber was used to treat 5 mm segments of seminal and nodal roots. This top view of the Plexiglas chamber shows the 300 μL receiver compartment, where a stable isotope exudation from the excised root end was measured. A 10 mm root segment extended to the 200 μL treatment compartment containing the isotope. The leakage check compartment was adjacent to the treatment compartment. (b) In <sup>32</sup>P experiments, a 15 mm segment of root extended from the 500 μL treatment compartment to the 300 μL receiver compartment and a 15 mm root segment was exposed to the treatment compartment. (c) In radial water loss experiments, the treatment compartment was always 30 mm from the apex and the solution was sampled from the receiver compartment and the compartment that corresponded to the sample position on the root (sample compartment).

position). Because of experimental constraints, root segments exposed to the treatment compartment could not be sampled, but a 5 mm root segment directly basally adjacent to the trimmed excised end was sampled, stored in 70% ethanol for root hair length and density phenotyping, acridine orange staining and anatomical analysis. The root was installed in a modified Pitman chamber (Hu *et al.*, 2014) (Fig. 1b) permitting treatment of a root segment with radionuclide. A 15 mm segment of root extended from the 500 μL treatment compartment to the 300 μL receiver compartment. The Pitman chamber compartments were isolated with silicon grease and filled with nutrient solution (protocol previously).

Immediately after installation of the root in the chamber, the solution in the treatment compartment was replaced with fresh nutrient solution containing approximately 10 μCi <sup>32</sup>PO<sub>4</sub>. After 45 min, the solution in the receiver compartment was discarded and replaced with 250 μL nutrient solution. After 10 min, the entire solution in the receiver compartment was collected. These sample times were determined by time course experiments sampling the receiver compartment 13 times at 5 min intervals by withdrawing the entire solution and replacing it with 250 μL of fresh nutrient solution (Fig. S1c). Acropetal movement of <sup>32</sup>P was checked by sampling 100 μL of the nutrient solution in

the leakage check compartment; data from chambers showing leakage were discarded. Samples were suspended in 15 mL gelling scintillation solvent (ScintiSafe Gel Cocktail, Fisher Scientific, Massachusetts, USA) and analysed by liquid scintillation spectroscopy (Perkin Elmer, Tri-Carb 3110 TR Liquid Scintillation Analyser, Massachusetts, USA). One-centimetre root samples were collected 3 cm from the apex of each individual root installed in the Pitman chamber and stored in 70% ethanol for acridine orange staining and anatomical analysis. In total, there were two replicates for each genotype and individual sample position exposed to the treatment compartment. Five positions on seminal roots (6, 18, 24, 36 and 48 cm from the apex) and three positions were sampled on nodal roots (3 cm, 8 cm, and 18 cm from the apex).

### Mannitol experiments

The purpose of these experiments was to measure the radial hydraulic conductivity of root segments in different osmotic pressures by varying the osmotic difference between the nutrient solution and xylem with the application of mannitol. These experiments were performed following the  $H_2^{18}O$  Pitman chamber protocol previously with minor modifications. The solution in the receiver compartment was collected 13 times at 5 min intervals after the  $H_2^{18}O$  treatment by withdrawing the entire solution and immediately weighing on an analytical balance. Mannitol (Sigma-Aldrich, Taufkirchen, Germany) concentrations of 20, 40, 50, 60 or 80 mosmol  $kg^{-1}$  in nutrient solution were added to the treatment compartment at 25 min after the  $H_2^{18}O$  treatment (Fig. S2). Osmolality of the nutrient solution and exuded xylem sap were analysed using an osmometer (Fiske Micro-Osmometer, Model 210, Fiske Associates, Massachusetts, USA). Root segments (5 mm in length) exposed to the treatment compartment and a 1 cm root segment 3 cm from the root apex were excised and stored in 70% ethanol for acridine orange staining and anatomical analysis. In total, there were three replicates for each genotype, individual sample position and mannitol concentration. Water isotopic analyses were carried out by the method described previously.

### Radial water loss

These experiments were performed to determine if radial water loss occurred along the root, including tissues with and without RCS. Radial water loss can be detected as isotope-labelled water leaking or moving radially through the cortex to outside the root. These experiments followed the  $H_2^{18}O$  Pitman chamber protocol previously with minor modifications. Radial water loss experiments were performed in three replications per genotype for each sample position, which consisted of nine positions on seminal roots (6, 12, 18, 24, 30, 34, 42, 48 and 54 cm from the apex) and four positions on nodal roots (3, 8, 13 and 18 cm from the apex). In these experiments, the treatment compartment was always 3 cm from the root tip. Twenty minutes after  $H_2^{18}O$  treatment; the solution in the receiver compartment was discarded and

replaced with fresh nutrient solution. After 10 min, the entire solution was collected from the compartment that corresponded to the sample position (sampling compartment) (Fig. 1c). The receiver compartment solution was also sampled. Root segments (5 mm in length) exposed to the treatment compartment, sampling compartment and a 1 cm root segment, 3 cm from the root apex, were excised and stored in 70% ethanol for acridine orange staining and anatomical analysis.

### Suberin analysis

The purpose of these experiments was to determine if increased aliphatic or aromatic suberin compounds coincided with RCS formation. Seminal and nodal roots were sampled at three positions along the length of the root [6–10 cm (distal), 20–24 cm (mid-root) and 34–38 cm (basal) from the root apex] in three replications per genotype from a solution culture grown plant at 35 DAG. These sample positions were chosen according to RCS formation; the distal segment had no RCS, the mid root segment had RCS formation and the basal section had maximal RCS or complete disappearance of the cortex. Surface areas of the endodermis and epidermis were estimated based on acridine orange staining and microscopy of root cross sections directly basally adjacent to selected sample positions. Suberin analysis was performed according to Schreiber *et al.* (2005) with the modification that enzymatic digestion of cell walls was performed prior to transesterification, and gas chromatography and mass spectrometry were used for suberin monomer analysis after transesterification, which is more precise than suberin staining, although not spatially explicit. Individual suberin monomers were identified through a homemade mass spectrometry suberin library. Barley does not develop a suberized exodermis, and therefore, suberin detected in this assay is endodermal suberin (Ranathunge *et al.*, 2017). Results of suberin analyses were expressed on the basis of total DW of original isolates used for the depolymerization, the surface area of the endodermis or root cross section (data not shown) and root segment length (data not shown) with similar results.

### STATISTICAL ANALYSIS

Data were analysed by linear regression, multiple regression, Pearson correlation coefficients, paired *t*-tests, ANOVA, Tukey's honest significant difference and a locally weighted polynomial using R 3.1.2 (R Core Team, 2014). Radial nitrate and water transport calculations were performed using a dilution equation  $[(\delta^{18}O \text{ sample} - \delta^{18}O \text{ tap water}) \times \text{xylem exudation } (\mu\text{L})] / (\delta^{18}O \text{ treatment} - \delta^{18}O \text{ tap water})$  where  $\delta^{18}O \text{ tap water} = -7.49$ . For radial phosphorus transport data, the counts per minute for  $^{32}P$  exudation in the treatment compartment were determined and normalized to counts  $\text{pmol}^{-1} P$ . The data were normalized to collection time (min) and surface area of the root exposed on the Pitman chamber (mm). Hydraulic conductivity was determined by dividing this value by the

differences in osmotic pressure between the nutrient solution and xylem sap (kPa).

## RESULTS

Root cortical senescence began in the outer cortical cell files and progressed inward. RCS increased in frequency basipetally. RCS can be visualized by the disappearance of the root cortex and the absence of acridine orange fluorescent nuclei. Seminal and nodal roots had the same pattern of RCS. Although epidermal cells became anucleate, they persisted much longer than the remainder of the cortex, often leaving only the epidermis, air space and then the stele (Fig. 2). For the duration of the experiment, the stele remained viable as determined through acridine orange fluorescent nuclei. RCS had the same pattern of programmed cell death in soil as in solution culture. At 35 DAG, plants grown in soil had 32 and 21% faster RCS development (defined as the greater percent cortical senescence) in seminal and nodal roots, respectively, compared with solution culture grown plants (Figs 3 & S3). Nutrient deficiencies did not influence where RCS formation began relative to the root apex, however, increased the rate of RCS formation (Fig. 4).

Genetic variation between landraces (Tkn24b and Nuernburg) and modern varieties (Arena and Golf) was observed for RCS in seminal and nodal roots. No significant differences between genotypes within the landraces or modern cultivar class were observed in RCS formation (Fig. S4). Landraces had a faster progression of RCS compared with modern varieties (Figs 3, 4 & S3). At 30 DAG, landrace nodal roots 8 cm from the apex had 51% RCS and seminal roots 8 cm from the apex had 56% RCS. In modern varieties, nodal roots 8 cm

from the apex had 30% RCS and seminal roots 8 cm from the apex had 32% RCS (Figs 3 & S3).

Nutrient deficiencies increased the rate of RCS in seminal and nodal roots. Nitrogen and P deficiency were confirmed through a 50% reduction in dry plant biomass and symptoms of chlorosis in nitrogen deficient plants and small dark leaves in phosphorus deficient plants (data not shown). Nitrogen and phosphorus stress increased the rate of RCS formation, however, did not affect the pattern of RCS (Figs 4 & S5). In LN, LP and control conditions, no RCS formed within 2 cm of the root apex or seed up to 45 DAG. At 35 DAG, landraces and modern varieties had 13% higher RCS development (i.e. greater percentage of cortical area senesced) in LP conditions and 11% higher in LN conditions compared with control conditions. At 35 DAG, 100% of the cortex had senesced at 18 cm from the apex in LN and LP conditions, compared with 85% senescence in control conditions (Fig. 4). In LP and LN conditions, RCS began developing approximately 5 d earlier compared with control conditions. Plants grown in suboptimal nutrient availabilities had 21% reduced root length. Therefore, data were also analysed based on relative distance from the apex to account for elongation rate differences in low nutrient availability conditions with similar results (Table S1).

Root cortical senescence coincided with reduced nutrient content of root tissue ( $\mu\text{mol cm}^{-1}$ ). Per centimetre root length, seminal and nodal root segments with RCS grown in control and LP conditions had significantly reduced P content compared with root segments with no RCS (Table 1, Fig. S6a). Root segments with maximal RCS, or complete disappearance of the cortex, grown in high-P and low-P conditions had 74% less P in seminal roots and 81% less P in nodal roots compared

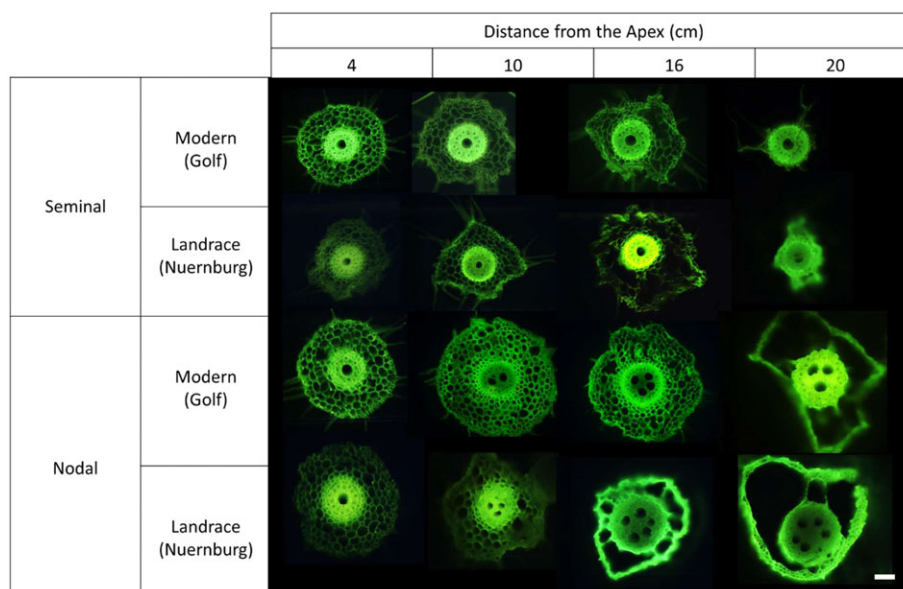


**Figure 2.** Seminal and nodal transverse cross sections of a landrace (Nuernburg) and modern variety (Golf) sampled at four positions on seminal and nodal roots at 35 DAG and stained with acridine orange. RCS increased in frequency basipetally. Nodal and seminal roots had the same pattern of RCS. Although epidermal cells became anucleate, they persisted much longer than the remainder of the cortex, often leaving the epidermis, air space and then the stele. Note that acridine orange nuclei are not visible in these images as they were located in deeper tissue layers, which were observed through confocal microscopy. Scale bar = 100  $\mu\text{m}$ .

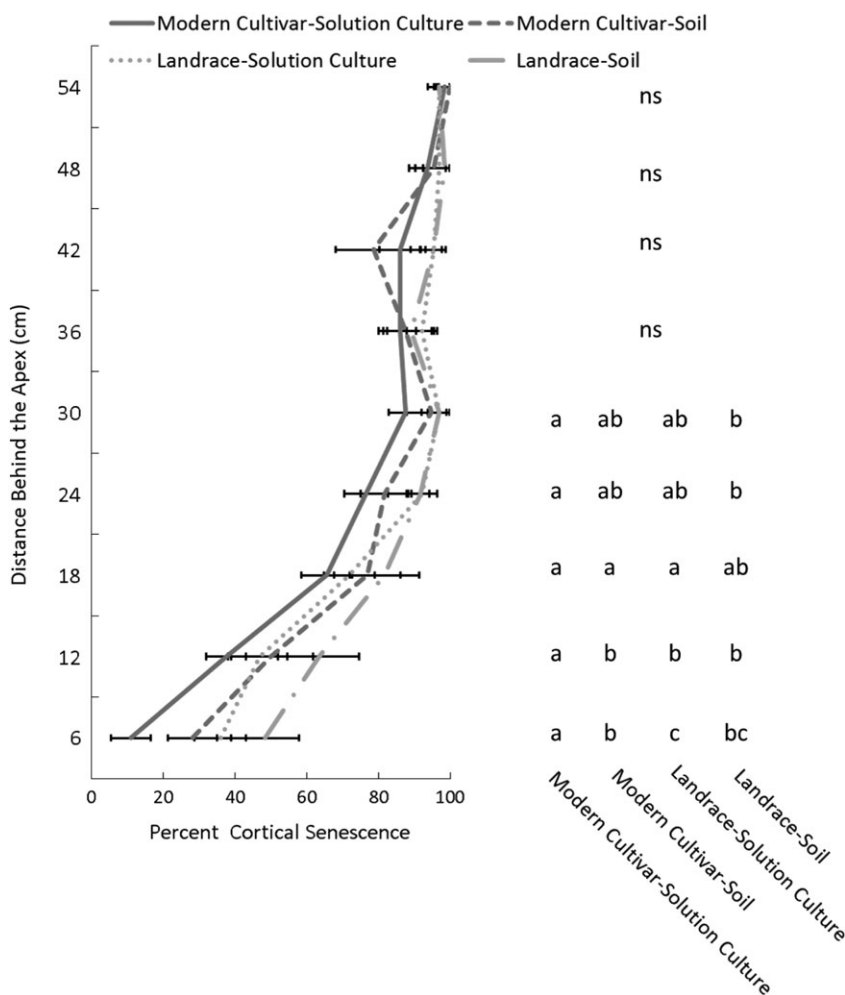


**Figure 3.** Root cortical senescence increased in frequency basipetally in soil and solution culture. Plants grown in soil had faster RCS development compared with solution culture grown plants. Data points are the mean of eight replications for seminal roots. Error bars represent standard error of the mean. Different letters represent significant differences within a sample position as determined by a Tukey's test ( $P < 0.05$ ). RCS was quantified by percent cortical senescence as determined by disappearance of cortical tissue compared with a non-senesced root segment on the same root.

with root segments with no RCS. Per gram of tissue, seminal root segments with maximal RCS had 19% less P in control conditions and low-P conditions compared with root segments with no RCS. Similar to seminal roots, nodal root segments with maximal RCS had 34% less P in control conditions and low-P conditions than root segments with no RCS.

As with P content, root N content was negatively correlated with RCS. Per centimetre root length, seminal roots grown in high-N and low-N conditions with maximal RCS had 73% less N compared with root segments with no RCS. Nodal roots grown in high-N and low-N conditions with maximal RCS had 79% less N compared with root segments with no RCS (Table 1, Fig. S6b). Per gram of tissue, seminal root segments with maximal RCS had 16% less N in high-N conditions and 19% less N in low-N conditions compared with root segments with no RCS. Nodal root segments with maximal RCS had 19% less N in high-N conditions and 12% less N in low-N conditions than root segments with no RCS per gram of tissue.

Roots with maximal RCS had 87% less respiration per unit root DW ( $\text{nmol O}_2 \text{ g DW}^{-1} \text{ sec}^{-1}$ ) than roots without RCS.

In seminal roots, maximal RCS formation was associated with reduced specific respiration in Arena by 78%, Golf by 91%, Nuernburg by 92% and Tkn24b by 95%. In nodal roots, maximal RCS formation was associated with reduced respiration per unit root biomass in Arena by 87%, Golf by 83%, Nuernburg by 92% and Tkn24b by 78% (Fig. S7). There was a significant negative correlation between RCS (as determined through a reduction in cortical tissue) and root respiration per unit biomass (correlation with log-transformed values,  $R^2 = 0.52$ ,  $P < 0.001$ ) (Fig. 5). Roots with maximal RCS had 96% less respiration per unit root length ( $\text{nmol O}_2 \text{ cm}^{-1} \text{ sec}^{-1}$ ) than roots without RCS. In seminal roots, maximal RCS was associated with reduced respiration per unit root length in Arena by 95%, Golf by 94%, Nuernburg by 98% and Tkn24b by 98%. In nodal roots, maximal RCS was associated with reduced respiration per unit root length in Arena by 96%, Golf by 95%, Nuernburg by 98% and Tkn24b by 93% (data not shown). RCS negatively correlated with root respiration per unit N ( $R^2 = 0.52$ ,  $P < 0.001$ ,  $\text{nmol O}_2 \mu\text{mol N}^{-1} \text{ sec}^{-1}$ ) and P ( $R^2 = 0.79$ ,  $P < 0.001$ ,  $\text{nmol O}_2 \mu\text{mol P}^{-1} \text{ sec}^{-1}$ ) (Fig. S8).

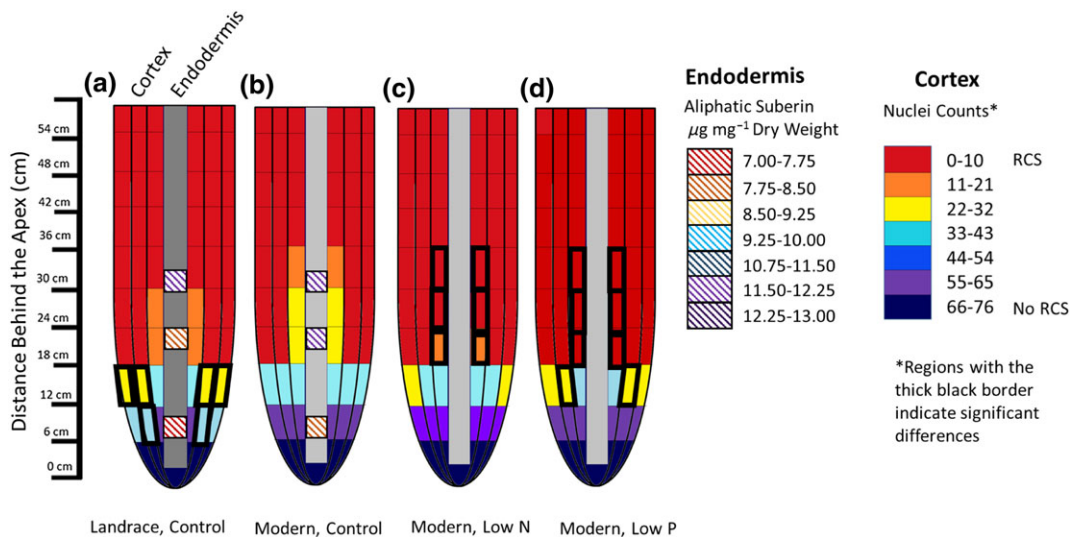


**Figure 4.** Effect of N and P on progression of RCS. The three cortical sections represent the inner, middle and outer cortical regions. (a) Progression of RCS and endodermal development in control conditions in a landrace. (b) Progression of RCS and endodermal development in control conditions in a modern cultivar. (c) Progression of RCS in low-N conditions in a modern cultivar. Nitrogen stress increased the rate, but did not affect the pattern of RCS development. (d) Progression of RCS in low-P conditions in a modern cultivar. Phosphorus stress increased the rate, but not the pattern of RCS. Colors of the cortex represent mean acridine orange fluorescent nuclei counts of 12 replications for seminal roots normalized for cell length in the three cortical regions. Cortical regions significantly different from a modern cultivar grown in control conditions (b) as determined by a paired *t*-test ( $P \leq 0.05$ ) are highlighted with a thick black border. Colors of the endodermis represent the mean aliphatic suberin in the endodermis of three replications for seminal roots in modern cultivars and landraces at three selected locations on the root.

**Table 1.** Linear correlations between RCS (percent cortex senesced) and nutrient content of seminal and nodal roots

Nutrient	Root class	Equation of line	95% CI intercept	95% CI slope	$R^2$		
P	Nodal	$y = -1.27e-04 \times + 1.22e-02$	5.09E-03	1.49E-02	-1.80E-04	0.53	
P	Seminal	$y = -3.25e-05 \times + 3.90e-03$	3.19E-03	4.62E-03	-4.64E-05	-1.86E-05	0.52
N	Nodal	$y = -1.69e-03 \times + 1.60e-01$	1.38E-01	1.96E-01	-2.26E-03	-1.12E-03	0.63
N	Seminal	$y = -4.96e-04 \times + 5.80e-02$	5.07E-02	6.53E-02	-6.37E-04	-3.43E-04	0.71

Root cortical senescence (x-axis: percent cortex senesced) reduces (negative slope) nutrient content of the root (y-axis:  $\mu\text{mol cm root length}^{-1}$ ) (Fig. S6). Per centimetre root length, RCS decreased N content in seminal and nodal roots grown in high N or low N. Per centimetre root length, RCS decreased P content in nodal and seminal roots grown in high P or low P. Data were fit to data points of two genotypes in four replications for three sample positions on seminal and nodal roots and two different nutrient applications ( $n = 96$ ). Differences between nutrient applications and genotypes were not significant and were combined for the analysis. Confidence intervals (CI) of coefficients are presented.

Hydraulic conductivity ( $\text{m s}^{-1} \text{MPa}^{-1}$ ) varied 18-fold in seminal roots and 21-fold in nodal roots (Fig. S9). There was a significant negative correlation between hydraulic conductivity and percent cortical senescence (correlation with log-transformed values,  $R^2 = 0.59$ ,  $P < 0.001$ , calculated across all genotypes because differences among genotypes were not significant) (Fig. 6a). Osmolality differences between the xylem and nutrient solution ranged from 0.103 to 0.114 MPa, with an average of 0.107 MPa. No univariate correlation was observed between radial water transport ( $\text{m s}^{-1}$ ) and the osmotic potential (Fig. S10). Nitrate transport rates varied 72-fold in seminal roots and 76-fold in nodal roots among genotypes (Fig. S11). There was a significant negative correlation between radial nitrate transport and percent cortical senescence (correlation with log-transformed values,  $R^2 = 0.58$ ,  $P < 0.01$ , calculated across all genotypes because differences among genotypes were not significant) (Fig. 6b).

Radial phosphorus transport rates varied among genotypes by 62-fold in seminal roots and 53-fold in nodal roots (Fig. S12). There was a significant negative correlation between radial  $^{32}\text{P}$  transport and percent cortical senescence (correlation with log-transformed values,  $R^2 = 0.64$ ,  $P < 0.001$ , calculated across all genotypes because differences among genotypes were not significant) (Fig. 6c). Root hair length and density had a significant effect on  $^{32}\text{P}$  uptake (data not shown). However, the additional surface area contributed by lateral roots and root hairs was found to be negligible (the few lateral roots and root hairs exposed to the treatment compartment had a very small diameter, and the maximum amount of lateral roots exposed to the treatment compartment would add less than 1% to the surface area, and the maximum amount of root hairs exposed to the treatment compartment would add less than 3% to the surface area), so these were ignored in the  $^{32}\text{P}$  transport calculations.

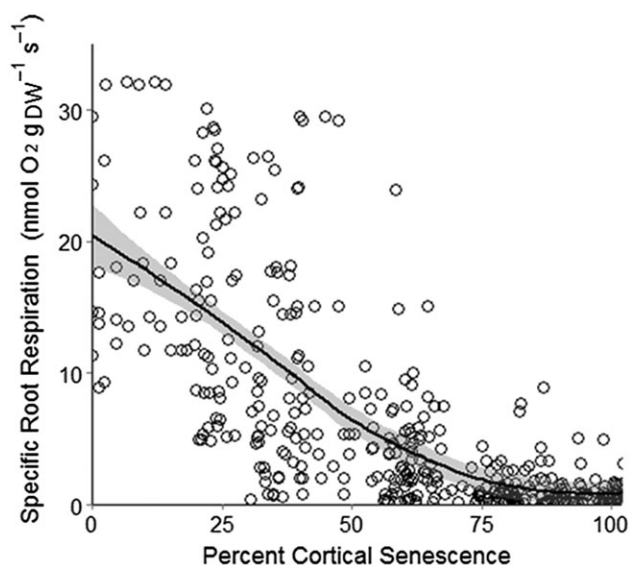


**Figure 5.** Negative relationship between specific root respiration and percent cortical senescence (seminal and nodal root data were combined because there were no relevant/significant differences between root classes or genotypes). Scatter plot with loess (locally weighed polynomial) line. Grey shading represents 95% confidence interval of loess line. A total of 416 data points from eight replications at nine sample positions on seminal roots and four sample positions on nodal roots from four genotypes are presented. Each symbol represents one data point. RCS was quantified by disappearance of the cortex compared with a non-senesced root segment on the same root.

The time course of water, nitrate and phosphate exudation into the receiver chamber demonstrated that there was a delay of approximately 10 min before tracer exudation was detected. Water and nitrate exudation stabilized around 20 min, and radial phosphate transport stabilized around 40 min after treatment (Fig. S1a–c). The greatest radial water, nitrate and phosphate transport rates occurred in the Arena and Golf genotypes followed by the Tkn24b and Nuernburg genotypes.

No radial water loss was detected at any sample position along the length of the root (Fig. S13a,b).  $H_2^{18}O$  concentrations in the receiver compartment were approximately  $9 \text{ m s}^{-1}$  in areas with no RCS (comparable with  $H_2^{18}O$  Pitman chamber experiments results; Figs S1 & S2). This is evidence that no detectable radial water loss occurred along the root in the Pitman chamber regardless of RCS development.

With increasing mannitol concentrations in the treatment compartment, a corresponding decrease in radial water transport was observed. Addition of 20, 40 or 50 mosmol  $\text{kg}^{-1}$  decreased radial water transport ( $\text{m s}^{-1}$ ) by 5, 25 and 36%, respectively. Mannitol concentrations of 60 mosmol  $\text{kg}^{-1}$  and greater resulted in no detectable radial water transport. As RCS progressed at increasing distances from the apex, no detectable radial water transport was observed (Fig. S2; data are presented only for nodal roots of the Golf genotype, other similar data not shown). Mannitol transport data are in agreement with xylem vessel potentials, and once the osmolality of the nutrient solution equalled the osmolality of the xylem sap, no transport was observed. This is evidence that the transport measurements from the Pitman chamber are due to

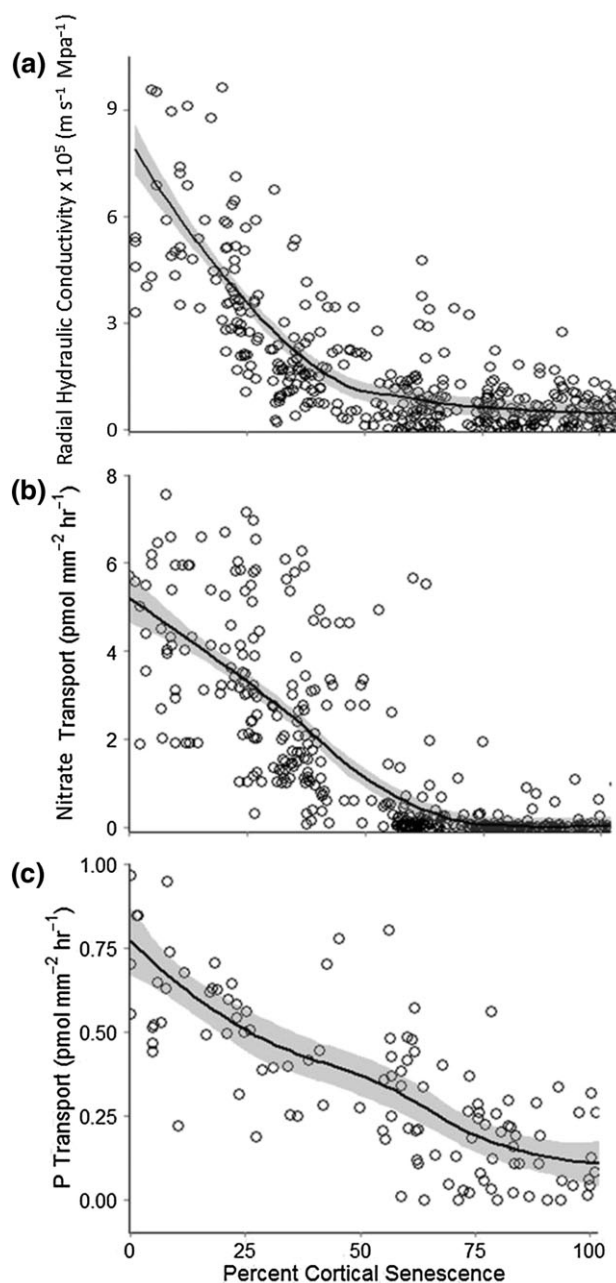


**Figure 6.** Negative relationships between radial nutrient and water transport and percent cortical senescence in seminal and nodal roots. (a) RCS was negatively correlated with hydraulic conductivity. (b) RCS was negatively correlated with radial nitrate transport. (c) RCS was negatively correlated with radial phosphorus transport. Grey shading represents 95% confidence interval of loess (locally weighed polynomial) line. Data from eight replications (a, b) and two replications (c) at each sample position are presented for both seminal and nodal roots for four genotypes. Seminal and nodal roots are not distinguished as no significant differences were detected. Each symbol represents one data point. RCS was quantified by disappearance of the cortex compared with a non-senesced root segment on the same root.

difference in osmotic potentials, with little contribution because of diffusion through the cortex.

In all samples, 16 suberin monomers were identified and divided into two groups: aromatic and aliphatic compounds.

Aromatic suberin on average comprised 53% of total suberin. Total suberin amounts between the distal, mid-root and basal sections were not significantly different. No significant differences were detected between landraces and modern varieties in the amount of aromatic suberin in the distal, mid-root and basal sections and aliphatic suberin in the distal or basal root sections. No significant differences were detected between genotypes within the landrace or modern cultivar groups in the amounts of aliphatic or aromatic suberin (Figs 7 & S14).

Landraces had 30% more ( $P < 0.05$ ) aliphatic suberin in mid-root sections compared with modern varieties (Figs 7a & S14). Omega hydroxy fatty acids ( $\omega$ -OH) comprised the majority (65%) of aliphatic suberin followed by diacids (23%), fatty acids (8.5%) and primary alcohols (2%), respectively. No significant differences were detected in the amount of  $\omega$ -OH in the basal portion of the root between landraces and modern varieties. Seminal and nodal roots of landraces had 37 and 26% more  $\omega$ -OH ( $P < 0.05$ ) at the mid-root section compared with

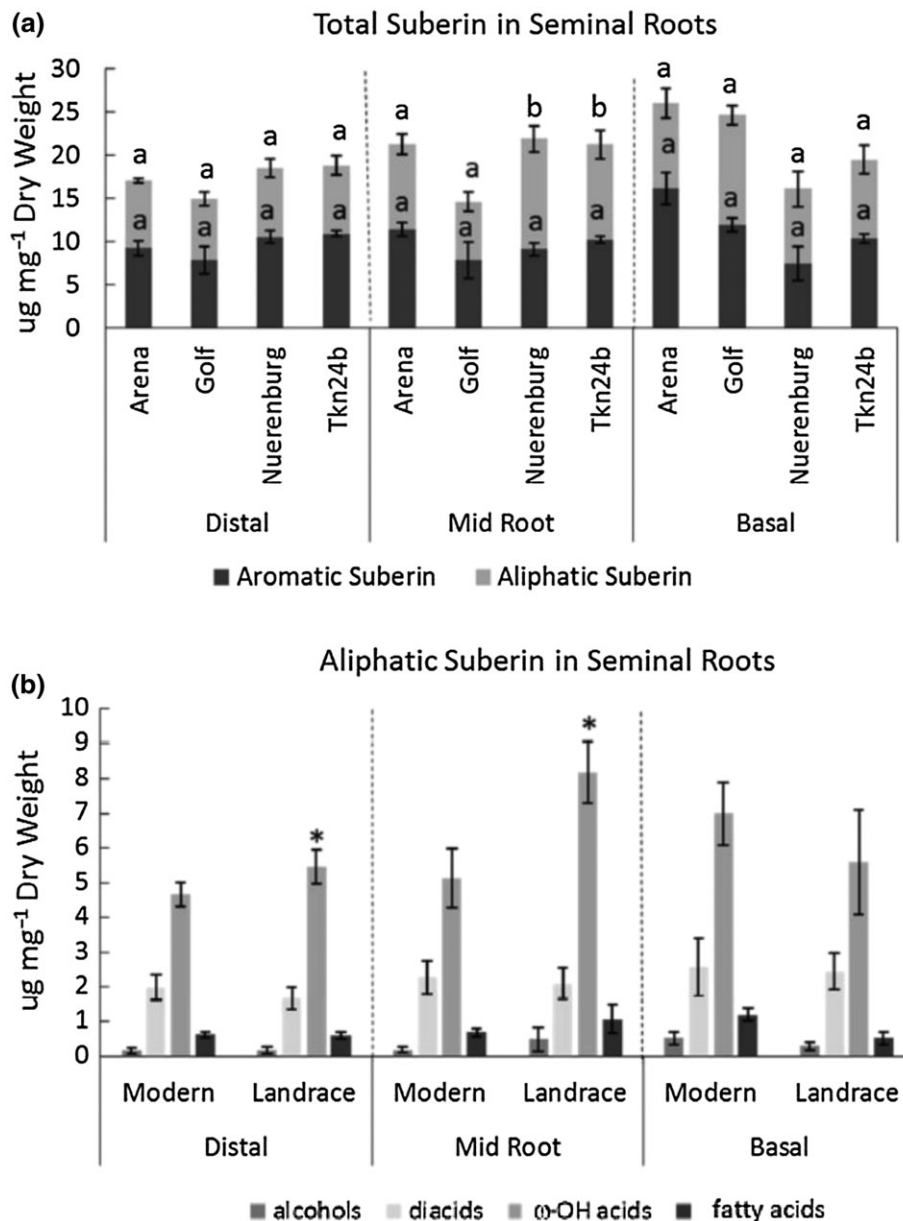


**Figure 7.** Suberin amounts in different segments of barley seminal roots. (a) Total suberin amounts in the distal, mid-root and basal root sections were not significantly different. Landraces had more aliphatic suberin in mid-root sections compared with modern varieties. Different letters represent significant differences within a panel as determined by a Tukey's test ( $P < 0.05$ ). (b) Omega hydroxy fatty acids comprised the majority of aliphatic suberin followed by diacids, fatty acids and primary alcohols, respectively. Landraces had more  $\omega$ -OH at the root apex and at the mid-root section compared with modern varieties. No significant differences were detected in the amount of  $\omega$ -OH in the basal portion of the root between landraces and modern varieties. Error bars represent standard error of the mean. Bars show means of three replicates of the two genotypes in each germplasm class  $\pm$  standard error (SE). Significance levels ( $*P \leq 0.05$ ) between landraces and modern varieties of a specific substance class in the same panel are shown as determined by a paired  $t$ -test.

modern varieties (Figs 7b & S14). This increase in  $\omega$ -OH corresponded with greater RCS development in mid-root regions (20 cm from the apex) of landraces compared with modern varieties (Fig. 3).

Few significant differences were found in chain length composition of the  $\omega$ -OH and diacid substance classes between genotypes in the distal, mid-root and basal sections of seminal roots (Fig. S15a–d). Few significant differences in chain length composition within  $\omega$ -OH and diacid substance classes were detected between the distal, mid-root and basal sections of individual genotypes of seminal and nodal roots (Figs S16 & S17). Nodal roots had similar results as seminal roots, and no differences were detected in total suberin between sample position or genotype (Fig. S14).

## DISCUSSION

To our knowledge, we present the first evidence for the physiological implications of RCS formation. Our results support our hypotheses, that is, (1) RCS reduces the respiration and nutrient content of root tissue (Figs 5 & S6, Table 1); (2) RCS reduces radial transport of water, phosphate and nitrate in excised seminal and nodal roots (Fig. 6a–c); (3) RCS coincides with increased aliphatic suberin in the endodermis (Fig. 7a,b). Significant variation for RCS exists in barley, and landraces had faster RCS formation compared with modern genotypes (Figs 3 & 4). Nutrient deficiency increased the rate of RCS formation (Figs 4 & S5), and we propose that accelerated RCS formation is not a stress symptom, but may be a useful adaptation under edaphic stress conditions. These results support the overall hypothesis that RCS reduces the carbon and nutrient costs of soil exploration and therefore is an important aspect of soil resource acquisition. RCS is associated with reduced radial water and nutrient transport to the stele, which has unknown functional implications although we speculate that reduced hydraulic conductivity may be advantageous under drought.

Genotypes varied in the development and rate of RCS (Figs 3 & 4). Landraces (Tkn24b, Nuernburg) had faster RCS compared with modern varieties (Arena, Golf), as previously reported by Liljeroth (1995). Historically, landraces are grown in low-input systems while modern varieties are typically selected using modern agronomic practices including irrigation and fertilization. This is circumstantial evidence that RCS could be useful for soil resource capture.

Root cortical senescence has been reported in several Triticeae species including wheat, triticale (*Triticosecale*), barley (Yeates and Parker, 1985; Liljeroth, 1995), rye (*Secale cereale*) (Deacon and Mitchell, 1985; Jupp and Newman, 1987) and oats (*Avena sativa*) (Yeates and Parker, 1985). RCS was not identified in maize (Wenzel and McCully, 1991). It is unclear whether additional species develop RCS. Species seem to differ in their propensity to develop RCS, in contrast to RCA, which is formed by many more species, including those which develop RCS. For example, barley and wheat have been shown to develop both RCS and RCA (Deacon and Mitchell, 1985; Setter and Waters, 2003). Our results indicate that RCS and RCA may have similar functions in reducing root

respiration and radial nutrient and water transport. They both are a form of programmed cell death, and it has been suggested that different environmental factors (e.g. hypoxia) induce programmed cell death via common mechanisms (Deacon *et al.*, 1986). The formation and progression of both RCA and RCS are accelerated by mineral nutrient deficiencies (Gillespie and Deacon, 1988; Drew *et al.*, 1989; Elliott *et al.*, 1993), and both RCA and RCS reduce root respiration (Fig. 5) (Zhu *et al.*, 2010; Saengwilai *et al.* 2014).

The patterns of programmed cell death in RCS and RCA are anatomically distinct. RCA formation begins in the mid-cortex and progresses radially outward (Kawai *et al.*, 1998), while in contrast, RCS consistently begins in the outer cortical cell regions and progresses inward (Figs 4 & S18, Henry and Deacon, 1981). The radial pattern of cell death during RCA formation leaves radial cortical cell connections between epidermis to the endodermis via hypodermis and stele, perhaps for transport of nutrients and water. In contrast, RCS largely disrupts the continuity of the cell-to-cell and apoplastic pathways to the stele, which depending on the growth medium (e.g. soil or solution culture) and what senesced cells are replaced with (e.g. air or water) may have important implications for water and nutrient transport from the soil to the stele. Additional studies are needed to further characterize the functional differences of RCS and RCA formation.

The root cortex fulfills important functional roles, and consequently, loss of the cortex during RCS may have negative implications for plant fitness. One such negative effect may be reduced mycorrhizal symbiosis caused by reduced cortical habitat. Inoculations with a vesicular-arbuscular mycorrhizal fungus delayed RCS development in wheat (MacLeod *et al.*, 1986), but no studies have been performed on the viability of mycorrhiza symbioses after RCS formation. The cortex is also thought to protect the root against pathogens (Holden 1976). Loss of the cortex may reduce the ability to sequester toxic ions, especially Na and Cl under salinity stress. As shown here, RCS also reduces radial transport of water and nutrients. Similar to RCS, although to a lesser extent, RCA formation in maize reduced radial nutrient transport (Hu *et al.*, 2014) and root hydraulic conductivity (Fan *et al.*, 2007). The reductions in nutrient transport and root respiration associated with RCA formation are less than what we measured here for RCS formation (Saengwilai *et al.* 2014; Hu *et al.*, 2014). The extent to which reduced nutrient transport associated with RCS is detrimental is uncertain, because RCS occurs in older root segments, whose rhizosphere may have been depleted of resources already. In this context, loss of the cortex represents a shift from a resource capture function of younger root tissue to supportive, axial transport and storage functions of mature root tissue.

In this study, large variability in radial water and nutrient transport was associated with variation in RCS (Fig. 6). Radial hydraulic conductivity values ranging from  $0.0005$  to  $0.011 \times 10^8 \text{ m s}^{-1} \text{ MPa}^{-1}$  for roots without RCS were in the same order of magnitude as presented in previous literature in barley in hydroponics ( $\sim 0.008\text{--}0.019 \times 10^8 \text{ m s}^{-1} \text{ MPa}^{-1}$ ) (Steudle and Jeschke, 1983) and rice in hydroponics ( $\sim 0.009\text{--}0.02 \times 10^8 \text{ m s}^{-1} \text{ MPa}^{-1}$ ) (Miyamoto *et al.*, 2001).

Nitrate showed the most significant reduction in transport with RCS. Radial nutrient and water transport across the cortex involves both the apoplast and cell-to-cell pathway, and ions can enter the cell-to-cell pathway via all cell types outside the endodermis (Tester and Leigh, 2001). Phosphate and nitrate are transported through the cell-to-cell pathway, and water is transported through both the apoplastic and cell-to-cell pathway. Formation of RCS could reduce nutrient transport through the cell-to-cell pathway by reducing the number and surface area of living cells between the epidermis and stele. In addition, cortical apoplastic radial pathways would have fewer intercellular routes after RCS formation. As RCS progresses, the continuity of the cell-to-cell pathway is increasingly disrupted. However, if cortical air spaces are lined or filled with an aqueous solution, ions could diffuse along the inside of the air spaces and be taken up by cortical cells, and the rate of movement of solutes towards the stele would be much faster (van der Weele *et al.*, 1996). It is important to note that the Pitman chamber method in this study drives water flow through osmotic differences, and at equilibrium, it only considers water flow through the cell-to-cell, not the apoplastic pathway. As roots with RCS often do not have an intact epidermis, it is very likely these air spaces are water filled, especially with solution culture grown plants. The sporadic occurrence of water filled or lined air spaces could account for some of the variability in the nutrient and water transport data.

We speculate that reduced hydraulic conductivity associated with RCS may be advantageous under water deficit by preventing desiccation of mature roots, the root tip and soil surrounding the root tip. Adequate hydration of the root tip and surrounding soil is important for continued root elongation. Under drought conditions, conservation of soil water throughout the growth season contributes to reproductive success (Lynch *et al.*, 2014). We speculate that reduced radial hydraulic conductivity and the elimination of the cortex caused by RCS may prevent desiccation of mature root tissue by reducing water flow from root to soil and may prevent desiccation of the root tip by reducing radial water loss from older root tissue, and by reducing internal water demand in the root. The decrease in hydraulic conductivity during the formation of RCS may be partly due to the suberization of the endodermis during RCS formation. RCS development corresponds to an increased aliphatic suberin content, specifically increased amounts of  $\omega$ -OH, the primary substance class in endodermal suberin, independently of tissue age (Fig. 7). Henry and Deacon (1981) propose that endodermal suberization and cell wall thickening restrict the movement of carbohydrates into the root cortex, thereby inducing RCS. However, in that study, RCS was not correlated with lignification in the Casparian strip or tertiary endodermis as assessed by phloroglucinol-HCl staining. In the present study, the formation of RCS coincided with increased suberin monomers. Increased  $\omega$ -OH content in the distal and mid-root sections of landraces corresponded to the early onset of RCS compared with modern varieties. It is not clear if increased suberization of the endodermis was the cause or effect of RCS or if they are associated by unknown mechanisms.

This increase in aliphatic suberin associated with RCS formation could have implications for water and nutrient transport. The amount of aliphatic suberin in roots was negatively correlated with the uptake of water in maize (Zimmermann *et al.*, 2000), water and Ca, Mn and Zn in *Arabidopsis* (Baxter *et al.*, 2009) and radial oxygen loss and oxygen permeability of rice roots (Kotula *et al.*, 2009a,b). However, some studies suggest that the endodermis may not always limit radial water flow. In *Arabidopsis*, the amount of aliphatic root suberin did not always negatively correlate with water and solute permeabilities (Ranathunge and Schreiber, 2011) and a disruption of the endodermis in young maize roots did not increase in radial hydraulic conductivity (Steudle & Peterson, 1998). Water uptake through suberized roots may be an important component of water capture, because in some species, unsuberized root surfaces are too short lived, absent or occupy too small of soil volume to supply all of the water and nutrients for plant growth. Significant uptake of water and nutrients was observed in suberized pine roots (Chung and Kramer, 1975), and in barley roots, suberized regions accounted for approximately half of the water taken up by the main axis (Sanderson, 1983). Little water enters the root through root meristematic regions (Frensch and Steudle, 1989) as xylem is not yet fully developed and functional in the root hair zone (McCully and Canny, 1988). In older regions of the root, the xylem is more developed and functional, but the endodermis may be suberized and lignified, limiting radial water transport. The increased aliphatic suberin content in the endodermis after RCS has developed could contribute to decreased radial transport of water and nutrients. From this study, it is unclear if passage cells in the endodermis are still present in older regions of the root after the cortex has senesced. After RCS has occurred, the passage cells would be the only cells capable of nutrient uptake and would provide areas of low resistance for water and nutrient movement through the endodermis. Additional studies are needed to further characterize the presence or absence of passage cells in the endodermis after RCS.

Our study focused on plants grown in solution culture and in soil. The majority of previous RCS studies focus on soil- and field-grown plants (Henry and Deacon, 1981; Lewis and Deacon, 1982; Wenzel and McCully, 1991; Elliott *et al.*, 1993; Liljeroth, 1995) in which roots may be easily damaged during excavation and washing. Previous studies used manual tissue sectioning (Yeates and Parker, 1985; Liljeroth, 1995; Bingham, 2007), which complicates the evaluation of tissue progressing towards senescence, because manual sectioning easily damages such tissue, and because it does not generate consistent section thicknesses for nuclei counts. In our study, roots were carefully sampled from rhizotrons to prevent the damage and sloughing off of the fragile epidermis and cortex that can occur when field-grown plants are excavated and washed.

In this study, we often found the epidermis to be intact long after the cortex had senesced and disintegrated, leaving an anucleate epidermis, air space and then the stele (Fig. 2). Cell wall modifications, like lignification and/or suberization, of the hypodermis and epidermal cell walls as described for several other species (Schreiber *et al.*, 1999) may allow this epidermal tissue of barley to persist longer than cortical parenchyma.

The use of solution culture-grown plants that were embedded and cryo-sectioned facilitated this observation (Fig. 2). Having an intact epidermis after RCS has progressed may have important implications in desiccation tolerance and or pathogen resistance of the root (Shane *et al.*, 2011).

In the present study, acridine orange staining was used to quantify RCS. Wenzel & McCully (1991) question the validity of acridine orange staining methods to assess nuclear viability in roots. However, the pattern of cell death and the relative rate of RCS development in different plant species were consistent among several cell viability assessments including acridine orange staining, single cell turgor pressure measurements, TUNEL-assay and Nomarski optics (Henry and Deacon, 1981; Wenzel and McCully, 1991; Liljeroth *et al.* 2001; Bingham, 2007). Because of the strong correlation between acridine orange staining and several other cell viability methods [e.g. Feulgen staining (Henry and Deacon, 1981) single cell pressure probe methods (Bingham, 2007)], we determined acridine orange staining to be a viable method for quantifying RCS.

We suggest that RCS could be an important trait for edaphic stress tolerance in crops. High-RCS genotypes had substantially reduced root respiration, root nutrient content and reduced radial phosphate, nitrate and water transport. Additional research is necessary in order to assess potential benefits and trade-offs of RCS for plant productivity. Most of the previous literature on RCS has focused on the formation of RCS in wheat; however, RCS development is similar in barley. We speculate that the functional implications and development of RCS in barley are analogous to wheat, triticale, rye and other grasses. We propose that RCS merits consideration as a trait for plant adaptation to edaphic stress.

## ACKNOWLEDGMENTS

We thank Christian Pfaff, Stella Eggels, Thomas Linnemann, Tanja Ehrlich, Vera Boeckem, Antonia Chlubek, Tania Galindo Castaneda, Michael Williams and Robert Snyder for technical support; Christian Kuppe and Wilfried Wolff for scientific and statistics support; and Holger Wissel for stable isotope analyses. This project was institutionally funded by the Hemholtz Association. Plant material was provided by IPK Gatersleben.

## REFERENCES

- Baxter I., Hosmani P.S., Rus A., Lahner B., Borevitz J.O., Muthukumar B., ... Salt D.E. (2009) Root suberin forms an extracellular barrier that affects water relations and mineral nutrition in *Arabidopsis*. *PLoS Genetics* **5**, e1000492
- Bingham I.J. (2007) Quantifying the presence and absence of turgor for the spatial characterization of cortical senescence in roots of *Triticum aestivum* (Poaceae). *American Journal of Botany* **94**, 2054–2058.
- Brand W.A., Coplen T.B., Vogl J., Rosner M. & Prohaska T. (2014) Assessment of international reference materials for isotope-ratio analysis (IUPAC Technical Report). *Pure and Applied Chemistry* **86**, 425–467.
- Brown M.E. & Hornby D. (1987) Effects of nitrate and ammonium on wheat roots in hnutobiotic culture: amino acids, cortical cell death and take-all caused by *Gaeumannomyces graminis* var. *tritici*. *Soil Biology and Biochemistry* **19**, 567–573.
- Chimungu J.G., Brown K.M. & Lynch J.P. (2014a) Reduced root cortical cell file number improves drought tolerance in maize. *Plant Physiology* **166**, 1943–1955.
- Chimungu J.G., Brown K.M. & Lynch J.P. (2014b) Large root cortical cell size improves drought tolerance in maize. *Plant Physiology* **166**, 2166–2178.
- Chung H.-H. & Kramer P. (1975) Absorption of water and <sup>32</sup>P through suberized and unsuberized roots of Lobolly Pine. *Canadian Journal of Forest Research* **5**, 229–235.
- Deacon J., Drew M. & Darling A. (1986) Progressive cortical senescence and formation of lysigenous gas space (aerenchyma) distinguished by nuclear staining in adventitious roots of *Zea mays*. *Annals of Botany* **58**, 719–727.
- Deacon J. & Mitchell R. (1985) Comparison of rates of natural senescence of the root cortex of wheat (with and without mildew infection), barley, oats, and rye. *Plant and Soil* **129–131**, 129–131.
- Drew M.C., He C.J. & Morgan P.W. (1989) Decreased ethylene biosynthesis, and induction of aerenchyma, by nitrogen- or phosphate-starvation in adventitious roots of *Zea mays* L. *Plant Physiology* **91**, 266–271.
- Elliott B., Robson A. & Abbott L. (1993) Effects of phosphate and nitrogen application on death of the root cortex in spring wheat. *New Phytologist* **123**, 375–382.
- Enstone D.E., Peterson C.A. & Ma F. (2003) Root endodermis and exodermis: structure, function, and responses to the environment. *Journal of Plant Growth Regulation* **21**, 335–351.
- Fan M., Bai R., Zhao X. & Zhang J. (2007) Aerenchyma formed under phosphorus deficiency contributes to the reduced root hydraulic conductivity in maize roots. *Journal of Integrative Plant Biology* **49**, 598–604.
- Frensch J. & Steudle E. (1989) Axial and radial hydraulic resistance to roots of maize (*Zea mays* L.). *Plant Physiology* **91**, 719–726.
- Gillespie I. & Deacon J. (1988) Effects of mineral nutrients on senescence of the cortex of wheat roots and root pieces. *Soil Biology and Biochemistry* **20**, 525–531.
- Henry C. & Deacon J. (1981) Natural (non-pathogenic) death of the cortex of wheat and barley seminal roots, as evidenced by nuclear staining with acridine orange. *Plant and Soil* **60**, 255–274.
- Holden J. (1976) Infection of wheat seminal roots by varieties of *Phialophora radiculicola* and *Gaeumannomyces graminis*. *Soil and Tillage Research* **8**, 109–119.
- Hu B., Henry A., Brown K.M. & Lynch J.P. (2014) Root cortical aerenchyma inhibits radial nutrient transport in maize (*Zea mays*). *Annals of Botany* **113**, 181–189.
- Huang B. & Nobel P.S. (1994) Root hydraulic conductivity and its components, with emphasis on desert succulents. *Agronomy Journal* **86**, 767–774.
- Jaramillo R.E., Nord E.A., Chimungu J.G., Brown K.M. & Lynch J.P. (2013) Root cortical burden influences drought tolerance in maize. *Annals of Botany* **112**, 429–437.
- Jupp A. & Newman I. (1987) Morphological and anatomical effects of severe drought on the roots of *Lolium perenne* L. *New Phytologist* **105**, 393–402.
- Kawai M., Samarajeewa P.K., Barrero R.A., Nishiguchi M. & Uchimiya H. (1998) Cellular dissection of the degradation pattern of cortical cell death during aerenchyma formation of rice roots. *Planta* **204**, 277–287.
- Kotula L., Ranathunge K., Schreiber L. & Steudle E. (2009a) Functional and chemical comparison of apoplastic barriers to radial oxygen loss in roots of rice (*Oryza sativa* L.) grown in aerated or deoxygenated solution. *Journal of Experimental Botany* **60**, 2155–2167.
- Kotula L., Ranathunge K. & Steudle E. (2009b) Apoplastic barriers effectively block oxygen permeability across outer cell layers of rice roots under deoxygenated conditions: roles of apoplastic pores and of respiration. *New Phytologist* **184**, 909–917.
- Lascaris D. & Deacon J. (1991) Relationship between root cortical senescence and growth of wheat as influenced by mineral nutrition, *Idriella bolleyi* (Sprague) von Arx and pruning of leaves. *New Phytologist* **118**, 391–396.
- Lewis S. & Deacon J. (1982) Effects of shading and powdery mildew infection on senescence of the root cortex and coleoptile of wheat and barley seedlings, and implications for root- and foot-rot fungi. *Plant and Soil* **69**, 401–411.
- Liljeroth E. (1995) Comparisons of early root cortical senescence between barley cultivars, Triticum species and other cereals. *New Phytologist* **130**, 495–501.
- Liljeroth E. & Bryngelsson T. (2001) DNA fragmentation in cereal roots indicative of programmed root cortical cell death. *Physiologia Plantarum* **111**, 365–372.
- Lynch J.P. (2013) Steep, cheap and deep: an ideotype to optimize water and N acquisition by maize root systems. *Annals of Botany* **112**, 347–357.

- Lynch J.P., Chimungu J.G. & Brown K.M. (2014) Root anatomical phenes associated with water acquisition from drying soil: targets for crop improvement. *Journal of Experimental Botany* **65**, 6155–6166.
- Lynch J., Epstein E., Lauchli A. & Weight G. (1990) An automated greenhouse sand culture system suitable for studies of P nutrition. *Plant, Cell & Environment* **13**, 547–554.
- MacLeod W., Robson A. & Abbott L. (1986) Effects of phosphate supply and inoculation with a vesicular-arbuscular mycorrhizal fungus on the death of the root cortex of wheat, rape and subterranean clover. *New Phytologist* **103**, 349–357.
- McCully M. & Canny M. (1988) Pathways and processes of water and nutrient movement in roots. *Plant and Soil* **111**, 159–170.
- Murphy J. & Riley J. (1962) A modified single solution method for the determination of phosphate in natural waters. *Analytica Chimica Acta* **27**, 31–36.
- Miyamoto N., Steudle E., Hirasawa T. & Lafitte R. (2001) Hydraulic conductivity of rice roots. *Journal of Experimental Botany* **52**, 1835–1846.
- North G.B. & Nobel P.S. (1995) Hydraulic conductivity of concentric root tissues of *Agave deserti* Engelm. under wet and drying conditions. *New Phytologist* **130**, 47–57.
- North G.B. & Nobel P.S. (1996) Radial hydraulic conductivity of individual root tissues of *Opuntia ficus-indica* (L.) Miller as soil moisture varies. *Annals of Botany* **77**, 133–142.
- Passioura J. (1988) Water transport in and to roots. *Annual Review of Plant Physiology* **39**, 245–265.
- Peterson C., Murrmann M. & Steudle E. (1993) Location of the major barriers to water and ion movement in young roots of *Zea mays* L. *Planta* **190**, 127–136.
- Postma J.A. & Lynch J.P. (2011a) Theoretical evidence for the functional benefit of root cortical aerenchyma in soils with low phosphorus availability. *Annals of Botany* **107**, 829–841.
- Postma J.A. & Lynch J.P. (2011b) Root cortical aerenchyma enhances the growth of maize on soils with suboptimal availability of nitrogen, phosphorus, and potassium. *Plant Physiology* **156**, 1190–1201.
- R Core Team. (2014) R: a language and environment for statistical computing.
- Ranathunge K. & Schreiber L. (2011) Water and solute permeabilities of *Arabidopsis* roots in relation to the amount and composition of aliphatic suberin. *Journal of Experimental Botany* **62**, 1961–1974.
- Ranathunge K., Kim Y.X., Wassmann F., Kreszies T., Zeisler V. & Schreiber L. (2017) The composite water and solute transport of barley (*Hordeum vulgare*) roots: effect of suberized barriers. *Annals of Botany* doi: 10.1093/aob/mcw252.
- Rasband, WS. ImageJ, U. S. National Institutes of Health, Bethesda, Maryland, USA, <http://imagej.nih.gov/ij/>, 1997–2016.
- Saengwilai P., Nord E.A., Chimungu J.G., Brown K.M. & Lynch J.P. (2014) Root cortical aerenchyma enhances nitrogen acquisition from low-nitrogen soils in maize. *Plant Physiology* **166**, 726–735.
- Sanderson J. (1983) Water uptake by different regions of the barley root. Pathways of radial flow in relation to development of the endodermis. *Journal of Experimental Botany* **34**, 240–253.
- Schreiber L., Franke R., Hartmann K.D., Ranathunge K. & Steudle E. (2005) The chemical composition of suberin in apoplastic barriers affects radial hydraulic conductivity differently in the roots of rice (*Oryza sativa* L. cv. IR64) and corn (*Zea mays* L. cv. Helix). *Journal of Experimental Botany* **56**, 1427–1436.
- Schreiber L., Hartmann K., Skrabs M. & Zeier J. (1999) Apoplastic barriers in roots: chemical composition of endodermal and hypodermal cell walls. *Journal of Experimental Botany* **50**, 1267–1280.
- Setter T.L. & Waters I. (2003) Review of prospects for germplasm improvement for waterlogging tolerance in wheat, barley and oats. *Plant and Soil* **253**, 1–34.
- Shane M.W., McCully M.E., Canny M.J., Pate J.S. & Lambers H. (2011) Development and persistence of sandsheaths of *Lyginia barbata* (Restionaceae): relation to root structural development and longevity. *Annals of Botany* **108**, 1307–1322.
- Steudle E. & Jeschke W. (1983) Water transport in barley roots. *Planta* **158**, 237–248.
- Steudle E. & Peterson C.A. (1998) How does water get through roots? *Journal of Experimental Botany* **49**, 775–788.
- Tester M. & Leigh R. (2001) Partitioning of nutrient transport processes in roots. *Journal of Experimental Botany* **52**, 445–457.
- van der Weele C.M., Canny M.J. & McCully M.E. (1996) Water in aerenchyma spaces in roots. A fast diffusion path for solutes. *Plant and Soil* **184**, 131–141.
- Wenzel C.L. & McCully M.E. (1991) Early senescence of cortical cells in the roots of cereals. How good is the evidence? *American Journal of Botany* **78**, 1528–1541.
- Yeates J.S. & Parker C.A. (1985) Rate of natural senescence of seminal root cortical cells of wheat, barley and oats, with reference to invasion by *Gaeumannomyces graminis*. *Transactions of the British Mycological Society* **86**, 683–685.
- Zhu J., Brown K.M. & Lynch J.P. (2010) Root cortical aerenchyma improves the drought tolerance of maize (*Zea mays* L.). *Plant, Cell & Environment* **33**, 740–749.
- Zimmermann H.M., Hartmann K., Schreiber L. & Steudle E. (2000) Chemical composition of apoplastic transport barriers in relation to radial hydraulic conductivity of corn roots (*Zea mays* L.). *Planta* **210**, 302–311.

Received 25 March 2016; received in revised form 28 January 2017; accepted for publication 3 February 2017

## SUPPORTING INFORMATION

Additional Supporting Information may be found online in the supporting information tab for this article.

**Figure S1.** Time course experiments to determine stable transport rates for sampling. A) Time course of  $\text{H}_2^{18}\text{O}$  Pitman chamber experiments.  $\text{H}_2^{18}\text{O}$  was detected 10 minutes after treatment. Stable transport rates were observed at 20 minutes after treatment. B) Time course of  $\text{N}^{18}\text{O}_3$  Pitman chamber experiments.  $\text{N}^{18}\text{O}_3$  was detected 10 minutes after treatment. Stable transport rates were observed at 20 minutes after treatment. C) Time course of  $^{32}\text{P}$  Pitman chamber experiments.  $^{32}\text{P}$  was detected 10 minutes after treatment. Stable transport rates were observed at 40 minutes after treatment. Time points with stable transport were selected as sample times for Pitman chamber experiments. Each line represents the transport of one seminal or nodal root through the duration of the experiment. As RCS progresses at increasing distances behind the root apex, radial water and nutrient transport decreases.

**Figure S2.** Mannitol time course experiments demonstrate decreasing radial water transport with decreasing osmotic differences between the nutrient solution and xylem at a: A) sample position 3 cm from the root apex, B) sample position 8 cm from the root apex, C) sample position 13 cm from the root apex, and D) sample position 18 cm from the root apex. Mannitol was applied at 25 minutes (represented by shaded area) and different mannitol concentrations are represented by different symbols. Each line represents the transport of one root. This figure shows a nodal root from the Golf genotype (data for other genotypes and root classes are similar (not shown)). With increasing mannitol concentrations in the nutrient solution the osmotic difference between the xylem and nutrient solution decreases, thus decreasing radial water transport. At increasing distances from the apex, radial transport was reduced because of the formation of RCS.

**Figure S3.** In nodal roots, RCS increased in frequency basipetally in soil and solution culture. Data points are the mean of eight replications and error bars represent standard error of the mean. Different letters represent significant differences within a sample position as determined by a Tukey's test ( $P < 0.05$ ). RCS was quantified by percent cortical senescence as determined by disappearance of cortical tissue compared to a non-senesced root segment on the same root.

**Figure S4.** RCS formation in A) nodal and B) seminal roots. Data points are the mean of eight replications and error bars represent standard error of the mean. Different letters represent significant differences within a sample position as determined by a Tukey's test ( $P < 0.05$ ). RCS was quantified by percent cortical senescence as determined by disappearance of cortical tissue compared to a non-senesced root segment on the same root.

**Figure S5.** RCS progression in nodal roots in A) control conditions in a landrace B) control conditions in a modern cultivar C) low N conditions in a modern cultivar D) low P conditions in a modern cultivar. The three cortical sections represent the inner, middle, and outer cortical regions. Colors of the cortex represent mean acridine orange fluorescent nuclei counts of twelve replications for seminal roots normalized for cell length in the three cortical regions. Cortical regions significantly different from a modern cultivar grown in control conditions (B) as determined by a paired t-test ( $P \leq 0.05$ ) are highlighted with a thick black border.

**Figure S6.** Negative relationships between root nutrient content and percent cortical senescence in seminal and nodal roots. A) Per cm root length, RCS decreased P content in nodal and seminal roots grown in HP and LP. B) Per cm root length, RCS decreased N content in nodal and seminal roots grown in HN and LN. No significant differences were observed in the fit of the line within each root class for plants grown in control or nutrient deficient conditions. Lines represent data fit linearly to data points of two genotypes in four replications for three sample positions on nodal and seminal roots (dashed line represents nodal linear fit and solid line represents seminal linear fit). RCS was quantified by disappearance of the cortex compared to a non-senesced root segment on the same root.

**Figure S7.** Negative relationship between specific root respiration and percent cortical senescence in A) seminal roots and B) nodal roots. Data from eight replications at each sample position are presented and genotypes are distinguished by different symbols. RCS was quantified by disappearance of the cortex compared to a non-senesced root segment on the same root.

**Figure S8.** Negative relationship between root respiration per unit N and P and percent cortical senescence in seminal and nodal roots. Data from four replications at each sample position are presented. RCS was quantified by disappearance of the cortex compared to a non-senesced root segment on the same root.

**Figure S9.** Negative relationship between radial hydraulic conductivity and percent cortical senescence in A) seminal roots and B) nodal roots. Data from eight replications at each sample position are presented and genotypes are distinguished by different symbols. RCS was quantified by disappearance of the cortex compared to a non-senesced root segment on the same root.

**Figure S10.** Relationship between water transport and the osmolality difference between the xylem and nutrient solution in nodal and seminal roots. Data from eight replications at each sample position are presented.

**Figure S11.** RCS was negatively correlated with radial nitrate transport. Data from eight replications at each sample position are presented for A) seminal roots and B) nodal roots. Each

symbol represents one data point and genotypes are distinguished by different symbols. RCS was quantified by disappearance of the cortex compared to a non-senesced root segment on the same root.

**Figure S12.** RCS was negatively correlated with radial phosphorus transport. Data from two replications at each sample position are presented for A) seminal roots and B) nodal roots for four genotypes. Each symbol represents one data point and genotypes are distinguished by different symbols. RCS was quantified by disappearance of the cortex compared to a non-senesced root segment on the same root.

**Figure S13.** Movement of  $H_2^{18}O$  into the sampling and receiver compartments of the Pitman chamber (See Fig. 1C for set-up). Radial water loss experiments to determine if RCS coincided with radial water loss of the root. Radial water loss along the length of (A) nodal root or (B) seminal roots of the Golf genotype. Each line represents the transport of one nodal or seminal root through the duration of the experiment. No isotope was detected 0 to 60 minutes after treatment at any sample location along the root. Radial water loss data for other genotypes and root classes are similar (not shown).

**Figure S14.** Suberin amounts in different segments of barley nodal roots. A) Total suberin amount in the distal, mid-root, and basal root sections. Different letters represent significant differences within a panel as determined by a Tukey's test ( $P < 0.05$ ). B) Omega hydroxy fatty acids comprised the majority of aliphatic suberin followed by diacids, fatty acids, and primary alcohols, respectively. Error bars represent standard error of the mean. Bars show means of three replicates of the two genotypes in each germplasm class  $\pm$  SE. Significance levels (\*,  $P \leq 0.05$ ) between landraces and modern varieties of a specific substance class in the same panel are shown as determined by a paired t-test.

**Figure S15.** Major aliphatic suberin substances,  $\omega$ -OH and diacids, for each genotype and sample position were analysed according to chain length. A) In the Golf genotype, C16 diacid amounts were significantly higher in the basal section compared to the distal and mid-root sections. B) In the Nuernburg genotype, C16, C20, and C26  $\omega$ -OH were significantly higher in the basal portion compared to the distal and mid-root sections. C) In the Arena genotype, C22 diacids were significantly higher in the basal portion compared to the distal and mid-root sections. D) The Tkn24b genotype had significantly higher C22 and C26  $\omega$ -OH in the mid-root section and significantly higher C22 diacids in the basal portion of the root compared to the distal sections. Data points are the mean of three replications. Error bars represent standard error of the mean. Significance levels (\*,  $P \leq 0.05$ ; \*\*,  $P \leq 0.01$ ) between landraces and modern varieties in the same panel are shown as determined through a paired t-test.

**Figure S16.** Major aliphatic suberin substances,  $\omega$ -OH and diacids, for each sample position were analysed in seminal roots according to chain length in individual genotypes. A) C16 diacids were significantly lower in the basal portion of Nuernburg genotype and C22 diacids in the Tkn24b genotype were significant higher in the basal portion compared to other genotypes. B) C26  $\omega$ -OH in the Tkn24b genotype was significant higher in the mid-root portion compared to other genotypes. C) No

significant differences of chain length composition within  $\omega$ -OH and diacid substance classes were detected between the distal sections of individual genotypes. Data points are the mean of three replications. Error bars represent standard error of the mean. Significance levels (\*,  $P \leq 0.05$ ; \*\*,  $P \leq 0.01$ ) between landraces and modern varieties in the same panel are shown as determined through a paired t-test.

**Figure S17.** In nodal roots, major aliphatic suberin substances,  $\omega$ -OH and diacids, for A) Basal; B) Mid-Root; and C) Distal sample positions were analysed according to chain length in individual genotypes. Data points are the mean of three replications. Error bars represent standard error of the mean.

Significance levels (\*,  $P \leq 0.05$ ; \*\*,  $P \leq 0.01$ ) between landraces and modern varieties in the same panel are shown as determined through a paired t-test.

**Figure S18.** Contrast between RCS and RCA. Barley transverse cross sections stained with acridine orange from plants 35 DAG grown in solution culture. A) RCS in nodal roots. RCS begins in the outer cortical cells, progresses inwards and often leaves an intact epidermis. B) RCA in nodal roots. RCA begins in the mid-cortex and has a radial pattern of cell death. Both RCS and RCA can be visualized by the disappearance of cortical tissue.